Surface Effects on Particle Self-Energies

H. Esbensen and G. F. Bertsch
National Superconducting Cyclotron Laboratory and Department of Physics-Astronomy, Michigan State University, East Lansing, Michigan 48824
(Received 16 April 1984)

The self-energy of a particle has a nearly singular behavior at a free surface of a Fermi liquid, as a result of the coupling to surface excitations. The imaginary part has a linear dependence on energy near the Fermi energy, whereas the effective mass shows a logarithmic divergence. The self-energy is calculated in semi-infinite nuclear matter with use of interactions constrained by self-consistency; the predictions are in qualitative agreement with experiment and more elaborate calculations for finite nuclei.

PACS numbers: 67.50.−b, 05.30.Fk, 21.60.Jz

In this Letter we examine the coupling of surface modes of a Fermi liquid to single-particle motion. The damping of the single-particle motion turns out to have a different analytic behavior than that arising from the coupling to bulk modes. We shall show how this comes about and then discuss the numerical application to nucleon propagation in nuclei. The theory of the particle self-energy is based on the perturbation-theory expression,[1]

$$\Sigma(\vec{r}_2,\vec{r}_1,\epsilon)=\int d\vec{r}_1'\int d\vec{r}_2'\int\frac{d\epsilon'}{2\pi}g_0(\vec{r}_2,\vec{r}_1,\epsilon')V(\vec{r}_1,\vec{r}_1')V(\vec{r}_2,\vec{r}_2')i\Pi^{\mathrm{RPA}}(\vec{r}_2',\vec{r}_1',\epsilon'-\epsilon). \tag{1}$$

Here g_0 is the single-particle Green's function in the Fermi liquid.[2] The Π^{RPA} is the RPA polarization propagator for the surface response. The polarization propagator differs from the ordinary causal RPA response only by the sign of its imaginary part.[2] In Eq. (1) V is an effective interaction that generates the RPA surface response from the noninteracting particle response. We studied the surface response of a Fermi liquid in detail previously.[3] We found that a useful approximation to the effective interaction is given by the separable function,

$$\begin{aligned}V(\vec{r}_1,\vec{r}_2)&=\int\frac{d^2\vec{K}}{(2\pi)^2}V(K,z_1,z_2)\exp[i\vec{K}\cdot(\vec{r}_1-\vec{r}_2)]\\&=\int\frac{d^2\vec{K}}{(2\pi)^2}\kappa(K)\exp[i\vec{K}\cdot(\vec{r}_1-\vec{r}_2)]\left.\frac{dV_0}{dz}\right|_{z_1}\left.\frac{dV_0}{dz}\right|_{z_2}.\end{aligned} \tag{2}$$

Our coordinate system is chosen with the surface in the x-y plane. Here V_0 is the mean-field potential of the Fermi liquid and $\vec{K}$ is a momentum vector along the surface of the liquid. The RPA polarization propagator is calculated from the usual noninteracting polarization propagator $\Pi^{(0)}$ by the equation

$$\Pi^{\mathrm{RPA}}=\Pi^{(0)}(1-V\Pi^{(0)})^{-1}. \tag{3}$$

We shall use the K,z representation of Π,

$$\Pi(\vec{r}_1,\vec{r}_2,\omega)=\int[d^2\vec{K}/(2\pi)^2]\exp[i\vec{K}\cdot(\vec{r}_1-\vec{r}_2)]\Pi(K,z_1,z_2,\omega).$$

The operator inversion in Eq. (3) reduces to algebraic division when the interaction has the separable form of Eq. (2). Because of the translational degeneracy of the surface position, the RPA response must diverge at zero frequency. This observation is used to fix the strength of the interaction, $\kappa(0)$. The K dependence of κ is closely related to the surface tension of the liquid.[4] We found in the nuclear case that a realistic-range interaction reproduced the empirical surface tension.[3] With the interaction specified by these considerations, the RPA response is found to have an approximate behavior at low frequencies given by

$$\int dz_1'\int dz_2'V(K,z_1,z_1')\Pi^{\mathrm{RPA}}(K,z_1',z_2',\omega)V(K,z_2,z_2')\cong\frac{V(K,z_1,z_2)}{\kappa(0)}\frac{1}{ia\omega-\sigma K^2}, \tag{4}$$

where a is a constant related to the noninteracting response, and σ is the surface tension. Note that Eq. (4) diverges at $K^2=0$, $\omega\rightarrow 0$, as required. From Eqs. (1) and (4) we may immediately deduce the analytic properties of Σ near $\epsilon-\epsilon_{\mathrm{F}}$. We first examine the imaginary part of the self-energy. When we evaluate Eq. (1)

for $\mathrm{Im}\Sigma$, it is found that only final states with energy between the initial energy and the Fermi energy contribute to the integral. The variation of g_0 near the Fermi energy can be ignored, leaving the following integral:

$$\mathrm{Im}\Sigma(\epsilon) \sim \left|\frac{\mathrm{Im}(\overline{g_0 V})}{\pi\kappa(0)}\right| \int_0^{\epsilon-\epsilon_F} d\omega \int \frac{d^2\vec{K}}{(2\pi)^2}\, \mathrm{Im}\left(\frac{1}{ia\omega - \sigma K^2}\right) = -\left|\frac{\mathrm{Im}(\overline{g_0 V})}{\pi\kappa(0)}\right| \frac{1}{8\sigma}(\epsilon-\epsilon_F). \tag{5}$$

The linear dependence on $\epsilon-\epsilon_F$ is to be contrasted with a quadratic dependence arising from the coupling to bulk modes.

The real part of the self-energy can be obtained from the Kramers-Kronig relation applied to the retarded self-energy Σ^{ret}, which differs from Σ in the sign of the imaginary part for energies above the Fermi energy. Thus $\mathrm{Im}\Sigma^{\mathrm{ret}}$ is nonanalytic at ϵ_F, which gives rise to a logarithmic behavior in the real part. These results are compared with some other examples of nonanalytic behavior in Fermi systems in Table I. In coupling of particles to the bulk modes of a Fermi liquid, the leading nonanalytic term in $\mathrm{Im}\Sigma^{\mathrm{ret}}$ is cubic,[5] giving a very weak logarithmic dependence to $\mathrm{Re}\Sigma$. In the Kondo effect,[6] particles couple to an isolated spin impurity, and $\mathrm{Im}\Sigma$ has a step-function behavior across the Fermi surface. This leads to an actual divergence in $\mathrm{Re}\Sigma$, observable in the impurity scattering cross section.

The nonanalytic behavior of the real self-energy implies that the effective mass of the particles diverges logarithmically at the Fermi energy

$$\frac{\bar{m}}{m} = 1 - \frac{\partial\Sigma(\epsilon)}{\partial\epsilon} \sim -\left|\frac{\mathrm{Im}(\overline{g_0 V})}{\pi\kappa(0)}\right| \frac{1}{4\pi\sigma} \ln|\epsilon-\epsilon_F|. \tag{6}$$

One consequence is that there should be a large surface contribution to the specific heat of the Fermi liquid near $T=0$.

We now turn to the application of Eq. (1) to the nucleon Green's function in a nucleus. The details of the calculation of Π^{RPA} are given in Ref. 3. To get some feeling for the applicability of the semi-infinite theory to the response in a finite system, we show in Fig. 1 a comparison of the RPA response for a typical wave number, $K \cong 0.3k_F$, with the RPA surface response of the nucleus ^{208}Pb. The corresponding spherical multipole in ^{208}Pb is $L = KR = 3$. In both response functions, there is a peak at low frequency. While the overall behavior of the response is reproduced including sum rules, the shell effects of the finite geometry are of course absent from the semi-infinite description. To calculate Σ we integrate the response function with the single-particle Green's function g_0, using the representation of g_0 in terms of the solutions of the Schrödinger equation.[7] The computation of $\mathrm{Im}\Sigma$ is straightforward, because all integrations are bounded. The integration for $\mathrm{Re}\Sigma$ involves unbounded K and ϵ integrations, and so the overall magnitude of $\mathrm{Re}\Sigma$ is somewhat model dependent—in fact, for a zero-range interaction, the integral diverges. We evaluate the expectation value of Σ in a single-particle wave function to extract a physical quantity. We choose the wave function as an eigenstate of the mean-field potential, with momentum perpen-

TABLE I. Nonanalytic behavior of self-energy in Fermi liquid.

Case	Leading nonanalytic $\mathrm{Im}\Sigma^{\mathrm{ret}}$	$\mathrm{Re}\Sigma$
Bulk modes[a]	$\lvert(\epsilon-\epsilon_F)\rvert^3$	$(\epsilon-\epsilon_F)^3\ln(\epsilon-\epsilon_F)$
Surface modes	$\lvert\epsilon-\epsilon_F\rvert$	$(\epsilon-\epsilon_F)\ln(\epsilon-\epsilon_F)$
Isolated spin[b]	$\theta(\epsilon-\epsilon_F)$	$\ln(\epsilon-\epsilon_F)$

[a]Ref. 5. [b]Ref. 6.

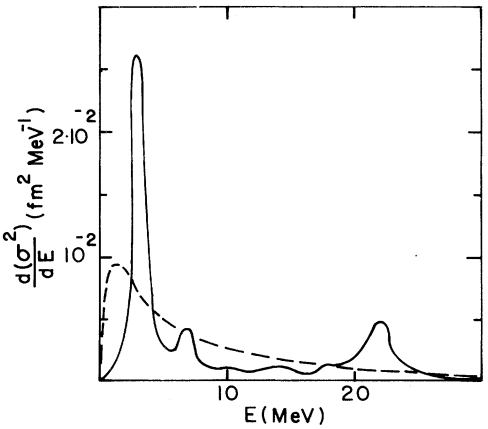

FIG. 1. Comparison of the isoscalar octupole response of ^{208}Pb (full drawn curve) and the surface response of a semi-infinite Fermi liquid (dashed curve). Both results are expressed in terms of the square of the zero-point amplitude of the surface position. The response of the semi-infinite system was calculated for a finite momentum transfer of $K \sim 3/R \sim 0.4$ fm^{-1}, compatible with the multipolarity of the finite-nucleus response.

dicular to the surface. The wave function is normalized in the interior of the medium to

$$\phi_k \sim 2^{-1/2}(e^{ikz}+R_i e^{-ikz}), \quad (7)$$

where R_i is a reflection coefficient. The expectation of Σ, calculated as

$$\langle\Sigma\rangle_k = \int dz_1 \int d^3r_2 \phi_k^*(\vec{r}_1)\Sigma(\vec{r}_1,\vec{r}_2,\epsilon_k)\phi_k(\vec{r}_2), \quad (8)$$

has the dimensions of energy times length. In Fig. 2 is shown the calculated imaginary part of Eq. (8). One physical quantity related to the imaginary self-energy is the probability of the particle making an inelastic collision with the surface. With our wave-function normalization, this probability is given by

$$P = k\Gamma_k/\epsilon_k \sim (k_F\Gamma_k/k)(0.04\ \text{MeV}^{-1}\ \text{fm}^{-1}), \quad (9)$$

where

$$\Gamma = 2\,\text{Im}\langle\Sigma\rangle_k. \quad (10)$$

is the decay rate of the state. Numerically, the probability of an inelastic reflection from the surface has a maximum of 100% for hole states ~ 10 MeV below the Fermi energy. Very deeply bound hole states are confined to the interior and do not interact strongly with the surface, but the bulk modes would become important at high excitation energies. The strong surface absorption implies that shell structure should be weak for hole states away from the Fermi energy, as is found empirically. A more quantitative way to compare with finite-nucleus properties is via Γ, the damping width of specific single-particle states. A wave function with momentum perpendicular to the surface corresponds to an s wave in spherical geometry; the normalization of the radial wave function in ^{208}Pb in the interior has the magnitude

$$|\phi_s|^2 \approx (1/R)|\phi_i|^2 \approx (0.1\ \text{fm}^{-1})|\phi_i|^2, \quad (11)$$

where R is the nuclear radius. The damping width obtained from Eqs. (10) and (11) and Fig. 2 has a peak of 2.3 MeV. Empirically, holes states have a width of 2–4 MeV for excitation energies between 5 and 10 MeV, and become much broader at higher excitation.[8] The calculated widths in ^{208}Pb associated with surface modes[9] are about 3 MeV for excitation energies between 5 and 10 MeV, in qualitative agreement with our result.

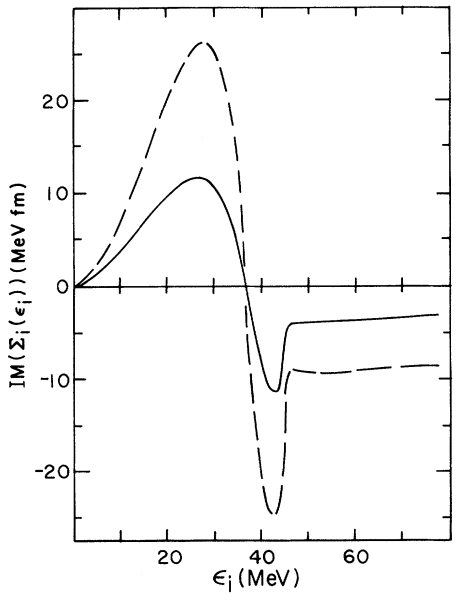

FIG. 2. The imaginary part of the self-energy of a particle moving perpendicular to the surface of a semi-infinite Fermi liquid. Results are shown as functions of the initial energy of the particle, both for an interaction with zero range along the surface (dashed curve), and for a finite range of 1 fm (full drawn curve).

For particles above the Fermi energy, the surface absorption is strong for barely bound orbits and decreases in the continuum. The continuum absorption is $\sim 25\%$ just above threshold. This is consistent with the empirical behavior of continuum nucleons. When a nucleon scatters from a nucleus, the effects of the wave propagation through the interior of the nucleus are readily apparent in the optical description.[10]

As discussed earlier, $\text{Re}\langle\Sigma\rangle$ has an $(\epsilon-\epsilon_F)\ \ln|\epsilon-\epsilon_F|$ behavior near the Fermi energy giving an infinite slope at $\epsilon=\epsilon_F$. The overall shape of $\text{Re}\langle\Sigma\rangle$ agrees qualitatively with the finite-nucleus calculations of Bortignon *et al.*[11] In both models, $\text{Re}\langle\Sigma\rangle$ has a sharp peak just above the Fermi energy, of magnitude 1–2 MeV.

The effective mass of nucleons near the Fermi surface has been the subject of much recent study. There are two contributions to the effective mass arising from the energy and momentum dependence of Σ. The energy dependence of the effective mass, Eq. (6), has been calculated in finite systems to have a peak $\bar{m}/m \approx 1.2$ at the Fermi energy.[9,12,13] The nonlocality of the mean-field potential gives a contribution in the opposite direction, so the overall effective mass is predicted to be close to one. Empirically, the systematics of compound-nucleus level densities demands an effective mass in the range $m^*/m \approx 1.2$–1.4 (Bohr and Mottelson[14] and Bertsch and Wu[15]), giving a significant discrepancy between theory and experiment. In our description, the effective mass diverges at ϵ_F as

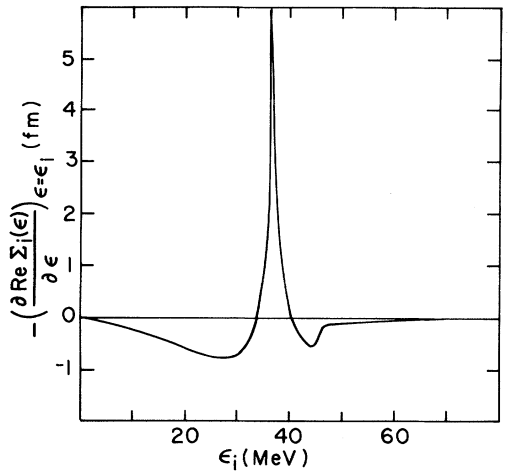

FIG. 3. The contribution to the effective mass extracted from the self-energy operator. The effective mass has a logarithmic divergence at the Fermi energy.

shown in Fig. 3, and only an average over some energy interval has physical significance. Using the normalization (11) and taking an energy interval $\Delta E \approx 4$ MeV corresponding to the lowest-frequency surface excitations, we find $\bar{m}/m = 1 - \Delta\,\mathrm{Re}\langle\Sigma\rangle/\Delta E \approx 1.2$ in agreement with the finite-system calculations. Perhaps for the statistical mechanics a more relevant energy scale is the temperature. Typical temperatures for the compound nucleus are of the order of 1 MeV, and over that interval the effective mass is larger, $\bar{m}/m \sim 1.4$.

We acknowledge discussions with P. F. Bortignon, which led to this study, and comments from W. J. Swiatecki. This work was supported by the National Science Foundation under Grant No. PHY-83-12245.

[1]There is a small correction to Eq. (1), in second-order perturbation theory, associated with overcounting the exchange interaction, which we have included in our numerical results. See G. Bertsch *et al.*, Phys. Lett. **80B**, 161 (1979).

[2]A. Fetter and J. Walecka, *Quantum Theory of Many Particle Systems* (McGraw-Hill, New York, 1971), Eq. (10.10) and Eq. (13.20).

[3]H. Esbensen and G. Bertsch, to be published.

[4]P. Feibelman, Ann. Phys. (N.Y.) **48**, 369 (1968).

[5]However, a more nonanalytic behavior obtains at the threshold of a bulk instability. See N. Berk and J. Schrieffer, Phys. Rev. Lett. **17**, 439 (1967); G. E. Brown *et al.*, J. Low Temp. Phys. **48**, 349 (1982).

[6]J. Kondo, Prog. Theor. Phys. **32**, 37 (1964). The theory beyond the perturbation result is reviewed by N. Andrei *et al.*, Rev. Mod. Phys. **55**, 402 (1983).

[7]C. Mahaux and H. A. Weidenmüller, *Shell Model Approach to Nuclear Reactions* (North-Holland, Amsterdam, 1969), p. 11.

[8]G. Bertsch, P. F. Bortignon, and R. A. Broglia, Rev. Mod. Phys. **55**, 287 (1983).

[9]P. F. Bortignon *et al.*, Phys. Lett. **108B**, 247 (1982).

[10]A. Bohr and B. Mottelson, *Nuclear Structure* (Benjamin, New York, 1969), Vol. 1, p. 165.

[11]P. F. Bortignon, R. A. Broglia, C. H. Dasso, and C. Mahaux, to be published.

[12]V. Bernard and N. Van Giai, Nucl. Phys. **A348**, 75 (1980).

[13]Z. Y. Ma and J. Wambach, Nucl. Phys. **A402**, 275 (1983).

[14]A. Bohr and B. Mottelson, *Nuclear Structure* (Benjamin, New York, 1969), Vol. 1, p. 188.

[15]G. Bertsch and J. Q. Wu, Michigan State University Cyclotron Laboratory Annual Report, 1982–1983, p. 62 (unpublished).